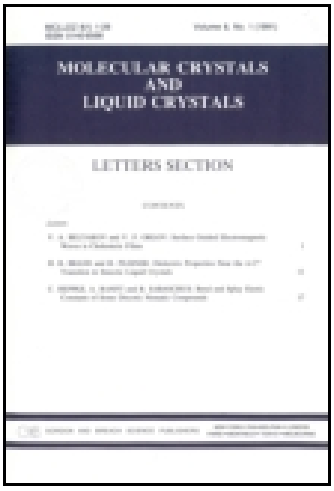

Molecular Crystals and Liquid Crystals
Publication details, including instructions for authors and subscription information:
http://www.tandfonline.com/loi/gmcl20

Preparation of Transparent Metal Films, Titanium-Doped Zinc-Oxide Films $(TiO_2)_2$ $(ZnO)_{98}$ on PEN by Using a RF-Magnetron Sputtering Method

Sungbo Seo[a], Yao Litao[a] & Hwamin Kim[b]
[a] Department of Electrical Engineering, Catholic University of Daegu, Gyeonsan, Republic of Korea
[b] Department of Advanced Energy Material Science and Engineering, Catholic University of Daegu, Gyeonsan, Republic of Korea
Published online: 06 Dec 2014.

To cite this article: Sungbo Seo, Yao Litao & Hwamin Kim (2014) Preparation of Transparent Metal Films, Titanium-Doped Zinc-Oxide Films $(TiO_2)_2$ $(ZnO)_{98}$ on PEN by Using a RF-Magnetron Sputtering Method, Molecular Crystals and Liquid Crystals, 602:1, 64-71, DOI: 10.1080/15421406.2014.940569

To link to this article: http://dx.doi.org/10.1080/15421406.2014.940569

Mol. Cryst. Liq. Cryst., Vol. 602: pp. 64–71, 2014

ISSN: 1542-1406 print/1563-5287 online
DOI: 10.1080/15421406.2014.940569

Taylor & Francis
Taylor & Francis Group

Preparation of Transparent Metal Films, Titanium-Doped Zinc-Oxide Films $(TiO_2)_2$ $(ZnO)_{98}$ on PEN by Using a RF-Magnetron Sputtering Method

SUNGBO SEO,[1] YAO LITAO,[1] AND HWAMIN KIM[2,*]

[1]Department of Electrical Engineering, Catholic University of Daegu, Gyeonsan, Republic of Korea
[2]Department of Advanced Energy Material Science and Engineering, Catholic University of Daegu, Gyeonsan, Republic of Korea

In this work, $(TiO_2)_x$ $(ZnO)_{100-x}$ (TZO) films were prepared on glass substrate at room temperature by RF-magnetron sputtering. The TZO film with $x = 2$ wt.% shows a very low resistivity of 4.7×10^{-4} Ω·cm which is comparable to that of ITO films and a high transmittance over 85% in the visible range. In particular, TiO_2 (2wt.%)-doped ZnO (TZO) films with thicknesses ranging from 100 ∼ 500 nm were also prepared on Polyethylene naphthalate (PEN) substrates under various RF-powers. Their electrical property were investigated as a function of RF-power. This property was found to be closely related with the crystallization and density of TZO films. It was also noted that vaporization of the water and other adsorbed particles, such as organic solvents contained in most plastic substrate affect the properties of the TCO films.

Keywords TiO_2-doped ZnO; thin film; reactive mode; TCO; flexibility

Introduction

Transparent and conductive oxide (TCO) films have been widely used as transparent electrodes for optoelectronics devices such as touch panels, flat-panel-displays (FPDs) and thin-film solar cells [1–15]. To date, doped oxides such as In_2O_3, SnO_2, and ZnO have been mainly used. However, these materials have often been limited in their application because they are chemically and thermally unstable in various environments [16–20]. In particular, amorphous silicon (a-Si) solar cells have received much attention as low-cost solar cells, but a higher conversion efficiency is needed for extensive use in power generating systems. If the conversion efficiency of an a-Si solar cell is to be improved, the stability of the TCO films used as a front electrode and an optical window layer is very important [21]. TCOs consist of a degeneration wide-band-gap semiconductor with a low electrical resistivity and a high transparency in the visible and the near-infrared wavelength range. Recently, ZnO has attractive interest as a conductive coating material because the material consist of cheap and abundant elements, is readily produced for large scale coatings, allows tailoring of the ultra violet absorption, has a high stability in a hydrogen plasma and has a low growth

*Address correspondence to H. M. Kim, Catholic University of Daegu, Hayang, Gyeongbuk 712-702, Korea (ROK). E-mail: hmkim@cu.ac.kr

temperature. In addition, the electrical resistivity of a ZnO thin film is readily modified by addition of impurities or by using reactive deposition [22–28].

In this work, titanium (Ti) doped zinc oxide (TZO) films were fabricated on the glass substrates by RF-magnetron sputtering [13–15]. Transparent metal films with lower resistivity were achieved by using $(TiO_2)_x$ $(ZnO)_{100\text{-}x}$ targets. The electrical and optical properties of the deposited TZO films were investigated as functions of film's thickness and composition ratio.

In addition, the durability of TZO films were also evaluated when the films were exposed to hydrogen plasma at various temperatures. These results were compared those of poly crystalline ITO (p-ITO) films.

On the other hand, the TZO films of x = 2 wt.% with the lowest electrical resistivity, were deposited on polyethylene naphthalene (PEN) for application to the flexible devices. Their electrical and optical properties were investigated as a function of applied RF-power. The electrical stability of TZO film against the damage due to the substrate bending was also investigated, the result was compared with that of ITO film

Experimental

The composite powders of $(TiO_2)_x$ $(ZnO)_{100\text{-}x}$, x = 1–5 wt.% were mixed by using ball mill for 24 hours with additional hand milling and were calcined at 600°C for three hours to remove the moisture 2 inch targets were made under a pressure of 12 tons by using a caver press and were solidified for each one hour at 250°C and 500 °C in Ar atmosphere. These sintered pellets were used as the sputter targets for TCO films. The substrates with a size of 50 × 50 mm^2 were cleaned sequentially by distilled water and alcohol, they were placed parallel to target surface at distance of 60 mm after achieving a base pressure of 10^{-5} Torr by using a diffusion pump. The TZO films, 100 ∼ 500 nm thick, were deposited on the glass substrates at room temperature under a pure Ar gas pressure of 1.2×10^{-3} Torr. Their electrical and optical properties were investigated as functions of the composition ratio and the applied RF-power. The crystalline phase of the deposited films were examined by wide angle XRD with thin-film attachments Cu Kα radiation ($\lambda = 0.154$ nm) and 0.02° angle steps were used. The film thickness were measured by using an α-step profiler (VEECO Co.) The surface and the cross sectional morphologies of the films were observed by using a scanning electron microscope (SEM, Hitachi Co.) and an atomic force microscope (AFM, Digital Instrument Co.).

The optical transmission spectra of the films were measured in the wavelength range from 200 nm to 1100 nm by means of an ultraviolet-near-infrared (UV-VIS) spectrophotometer (Shimadzu Co.). It was confirmed from an electron prove micro-analyzer (EPMA, Shimadzu Co.) that the composition ratios of the deposited films were almost consistent with those of the target. On the other hand, to investigate the durability when exposed to a hydrogen plasma, we used 200-nm-thick TZO film with x = 2 wt.%. This film was placed on the surface of a cathode in a plasma enhanced chemical vapor deposition (PECVD) chamber that could deposit an amorphous Si film in a practical manner. The hydrogen plasma was generated under a H_2 gas pressure of 20 mTorr and a RF-power of 60 mW/m^2. The films were exposed to hydrogen plasma for thirty min at various temperature from 100°C to 300°C and their durability was evaluated as changes in the optical transmittance and the electrical resistivity. The durability was compared to that of a commercial poly-crystalline ITO (p-ITO) film with a thickness of 200 nm that has been already reported in previous work. Also, in the test of the bending effects for TZO films, deposited on PEN

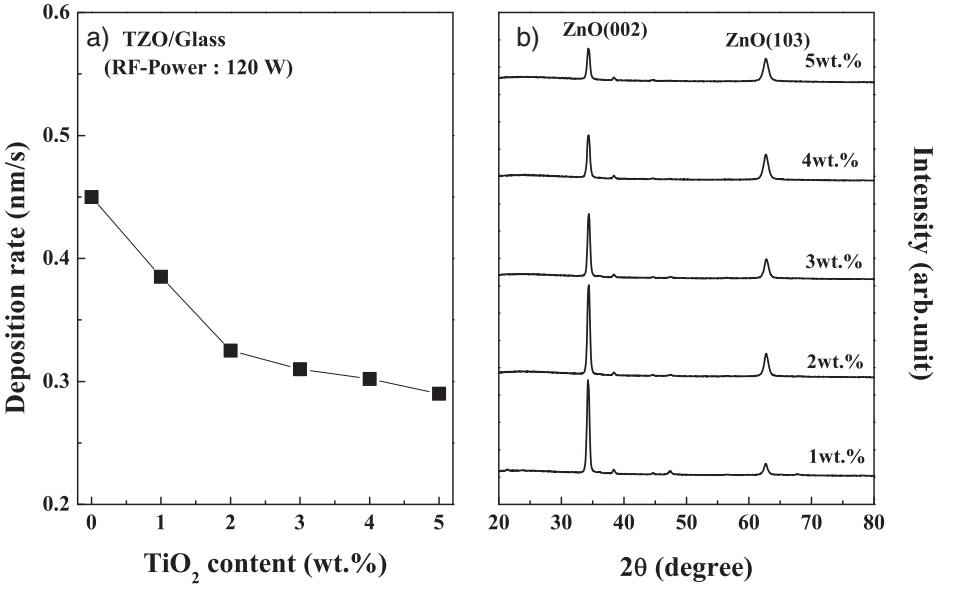

Figure 1. (a) Deposition rate of TZO films as a function of TiO_2 content. (b) X-ray diffraction patterns for TZO films with different TiO_2 content.

substrates, the substrates were bent around a cylinder of radius R, and the changes in sheet resistance were examined.

Results and Discussion

Figure 1(a) shows the deposition rate as a function of TiO_2 content for TZO films deposited on glass substrates by a RF-power of 120 W. The deposition rate decreases with increasing TiO_2 content. This is because the sputtering yield of TiO_2 is smaller as compared with ZnO. For the films corresponding to each of the TiO_2 content, their thickness can be controlled by using the deposition rate and the deposition time And Figure 1(b) shows X-ray diffraction patterns of 500-nm-thick TZO films with different TiO_2 content. It can be seen that only the diffraction peaks (002) and (103) are observed for all the TZO thin films, which have an obvious highly c-axis orientation. However, the intensity of (002) peaks gradually decreases and broadens with increasing TiO_2 content from 2 wt.% up to 5 wt.%. It reasoned that the crystallinity of TZO film decreased with increasing TiO_2 content. In particular, over x = 5 wt.%, the crystalline peaks so small we could not observed. Therefore it is obvious that the microstructure of TZO films depends on the composition ratio. That is, as TiO_2 content is increased, TZO films are amorphised.

Figure 2(a) shows the sheet resistance changes as a function of thickness for various TZO films on the glass substrates at room temperature, where an applied RF-power was 100 W. In general, the sheet resistance, inversely proportional to the film's thickness. For instance, $R_s = \rho/t$, where ρ and t are the electrical resistivity and the film's thickness, respectively. Thus, the sheet resistance remarkably decreases with increasing thickness for TZO films with a same TiO_2 content while for TZO films with a same thickness, the lowest sheet resistances are obtained in the films with x = 2 wt.%. However, for over x = 2 wt.%, the sheet resistance increases as the TiO_2 content increases. On the other hand,

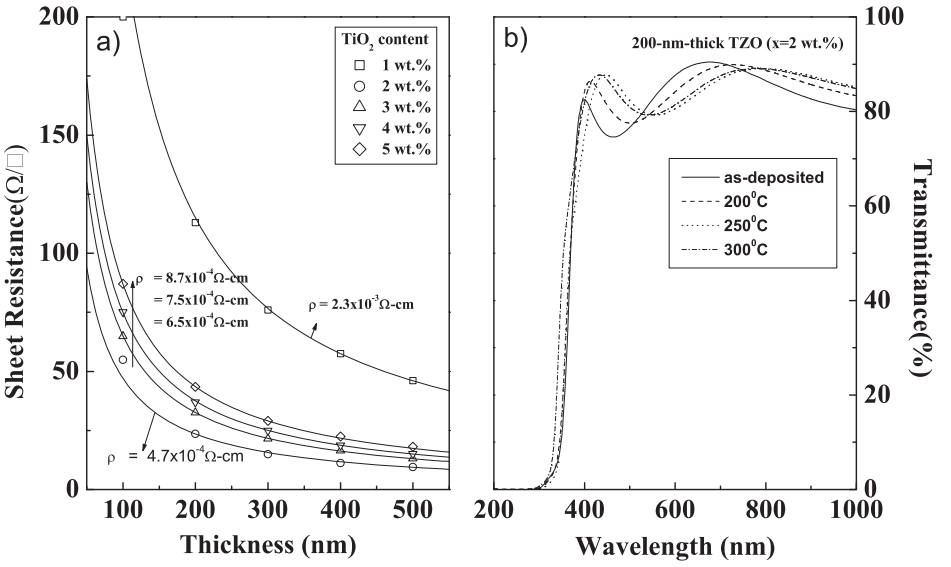

Figure 2. (a) Sheet resistance changes as a function of thickness for TZO films with different TiO_2 concentrations deposited on glass substrates at room temperature by RF-power of 120 W, where the solid lines indicate theoretical sheet resistance of TZO films. (b) Optical transmittance changes for 200-nm-thick TZO film with x = 2 wt.% exposed to a hydrogen plasma for thirty minutes at various temperatures.

in Figure 1, the solid lines indicate the theoretical resistances as a function of film's thickness that were fitted by a typical resistivity (ρ), using the equation of $R_s = \rho/t$. It is shown that the theoretical values are in good accord with the experimental values in the films with thickness of more than 200 nm. TZO film with x = 1 wt.% shows the most poor electrical conductivity, while the lowest resistivity of 4.7×10^{-4} Ω·cm is obtained in a TZO film with x = 2 wt.%. However, the resistivity increases with increasing TiO_2 content for over x = 2 wt.%. This resistivity increase may be closely related the microstructure of the TZO films, as shown in Figure 1(b). In general, the amorphous TZO films have a smaller mobility than the crystalline TZO films.

Therefore, we hypothesized that the resistivity increase in the TZO films with increasing TiO_2 content is a result of the decrease in the mobility due to a phase transformation of the films from a crystalline phase to an amorphous phase with increasing TiO_2 content. Figure 2(b) shows optical transmittance changes for 500-nm-thick TZO film with x = 2 wt.% after they were exposed to a hydrogen plasma for thirty min at various temperatures. It was found in the previous work [28] that the transmittance of a p-ITO film decreased significantly as the temperature was increased when the ITO film were exposed to a hydrogen plasma for thirty minutes at various temperatures, in particular, the transmittance dropped to 20 ∼ 30% and the conductivity also decreased after being exposed to a hydrogen plasma for thirty minutes at 300°C. However, in the case of the TZO films, there was no optical loss, but the absorption edge was blue shifted due to hydrogen incorporation into the film, indicating the Burstein Moss effect, as shown in Figure 2(b). The TZO films showed very excellent optical and electrical stabilities when they were exposed to hydrogen plasma. We, therefore, suggest that TZO films are sufficiently transparent and have a high enough conductivity and excellent durability under the hydrogen plasma so that they can be applied to TCO films for displays and a-Si solar cells.

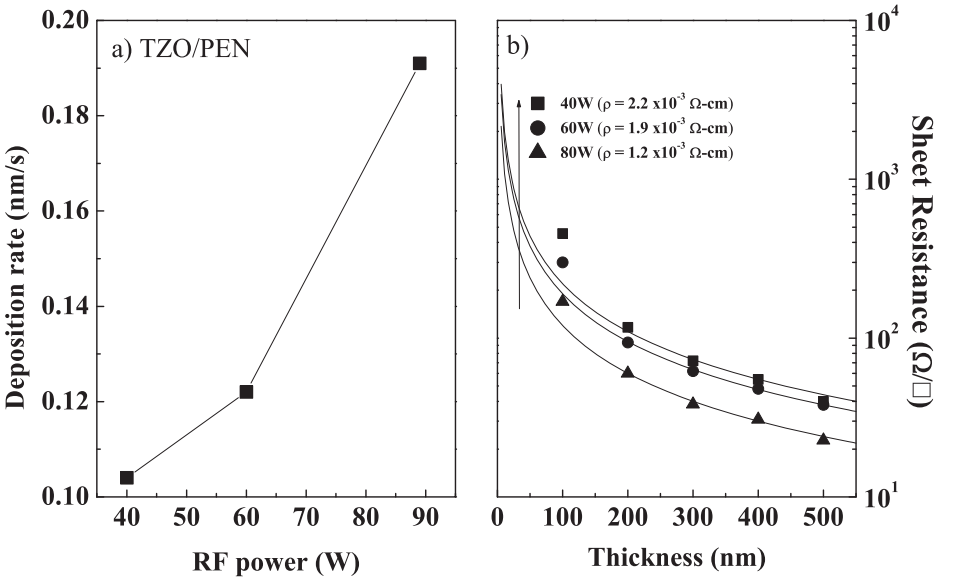

Figure 3. (a) Deposition rate as a function of RF-power and (b) sheet resistance changes as a function of film thickness, where the solid lines indicate theoretical sheet resistance fitted to the measured sheet resistance for TZO films with x = 2wt.% deposited on PEN substrates.

In this work, the TZO films with x = 2 wt.% were also deposited on the polyethylene naphthalate (PEN) substrates, and their deposition characteristics and electrical property were investigated as a function of applied RF-power. The results are shown in Figure 3. The deposition rate increases remarkably with increasing RF-power, as shown in 3 (a). By using this deposition rate, the film's thicknesses corresponding to each of the applied RF-power were determined by controlling the deposition time. For the TZO films deposited on PEN under different RF-powers, the sheet resistance as a function of film thickness were also plotted in Figure 3(b). The thickness dependence on the sheet resistance of TZO film was already described in Figure 2, and the theoretical resitivities fitted from the equation ($R_s = \rho/t$) between the sheet resistance and film thickness, were also shown in Figure 3(b). The lowest resistivity of 1.2×10^{-3} Ω·cm was obtained in a TZO film deposited under the RF-power of 80 W. However, this resistivity is much larger than that of the film deposited on the glass, shown in Figure 2(a). Because the PEN substrate contains water vapor or other adsorbed particles, such as organic solvents, vaporization of these particles deteriorates the adhesion of the TZO film to the PEN substrate. Mixing of these vaporized gases in the sputtering process will also affect the electrical property of the deposited TZO films. If a proper gas barrier is coated on the PEN substrate, it would be reasonably expected to suppress the diffusion of vapors from the substrate so that a TZO film with an improved quality might be obtained.

On the other hand, in Figure 3(b), it is notable that the RF-power have a significant impact on the electrical property of TZO films. In other words, the sheet resistance of TZO film decreases with increasing RF-power for TZO films with a same thickness, in particular, the decrease becomes more noticeable in the thickness below 200 nm. Such a sheet resistance difference with RF-power originates mainly from the different deposition rates. It may be attributed to the difference in the adatom mobility and resulting surface diffusion during the film growth. It is generally considered that the adatoms have a lower

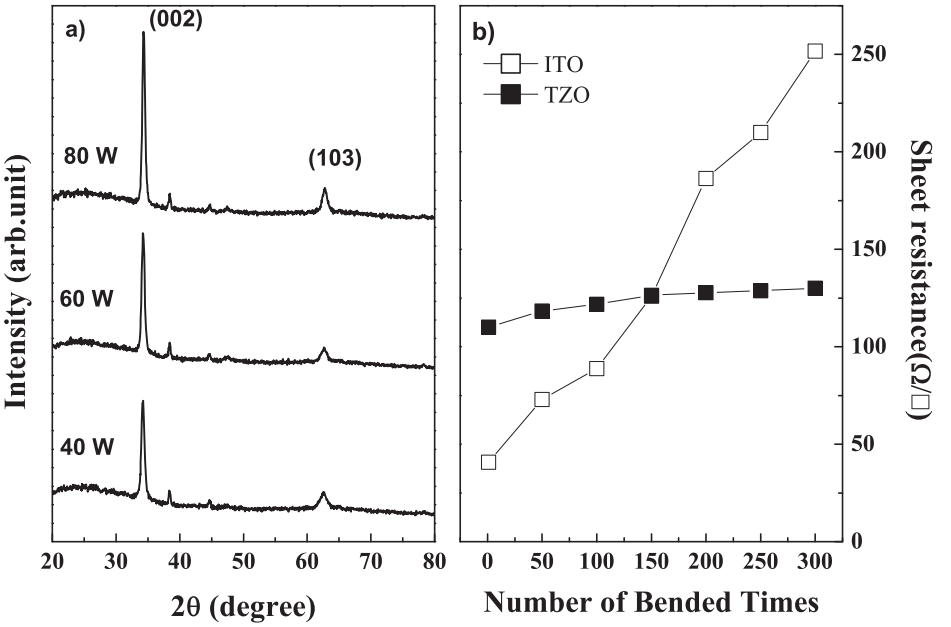

Figure 4. (a) X-ray diffraction patterns of 200-nm-thick TZO films deposited on PEN substrate under different RF-powers and (b) the sheet resistance changes as a function of bending times around a cylinder with a bending radius of 9 mm for ITO and TZO films with a thickness of 200 nm deposited on PEN substrates by 80 W.

mobility as the RF-power is lower, which results in low-density films since the adatoms with the lower mobility are condensed as soon as they reach on the substrate. In contrast, the adatoms have relatively higher mobility under the higher RF-power, which enhances their surface migration in sputtering process, thus inducing a higher density. These results can be also confirmed in Figure 4, for XRD patterns of TZO films deposited on PEN.

Figure 4(a) shows XRD patterns for 200-nm-thick TZO films deposited on PEN under different RF-powers. All films showed a similar pattern, containing two crystalline peaks corresponding to the (002) and the (103) peaks. The intensity of the (002) peak increased with increasing RF-power. This means that the crystalline phase increased in the TZO films with increasing RF-power. The grain size was calculated from the XRD patterns of Figure 4, using Scherrer formular

$$\mathrm{D} = 0.9\lambda/(\beta \cos\theta) \tag{1}$$

where λ (0.154 nm) is wavelength of X-ray (Cu Kα), β is full width at half maximum (FWHM) of (002) peak, and represents the grain size. The calculated grain size was also shown in the Figure 4(a). The grain size was found to be increased from 16.1 nm to 28.2 nm with increasing RF-power. This means that the TZO films are more crystallized with increasing RF-power. Therefore, the resistivity decrease with RF-power, as shown in Figure 4(b), is caused by the mobility increase due to crystallization of the TZO film. In general, since the conventional sputter apparatus has a system of the target and the substrate facing with each other, the particles with high energy such as γ-electrons, neutral Ar particles, and negative oxygen ions collide with the substrate. Therefore, when the

TZO films are deposited on the polymer substrate by the conventional sputter technique, the bombardment of energetic particles and thermal heat generated during the sputtering process can result in damage to the underlying polymer substrate [9]. We, therefore, suggest that the applied RF-power should be as large as possible within a range that does not damage the polymer substrate to obtain TZO films of high quality on the polymer substrates by using RF magnetron sputtering. In Figure 4(b), we present the sheet resistance change as a function of the number of bending times for 200-nm-thick TZO film prepared on PEN by 80 W. For comparison, that of ITO (In_2O_3 : SnO_2 = 90 : 10 wt.%) with a thickness of 200 nm prepared by 80 W, is also shown. Here, the PEN substrates are positively bent around a cylinder with a radius of 10 mm. Compared to ITO film, the TZO film shows a poor electrical conductivity, while a superior electrical stability due to the bending stress.

Conclusions

In this work, TZO films with composition ratios of $(TiO_2)_x$ $(ZnO)_{100-x}$, x = 1, 2, 3, 4, 5 wt.% were fabricated on slide glass at room temperature by using RF magnetron sputtering method. Their electrical resistivity was investigated as a function of the TiO_2 content. The lowest resistivity of 4.7×10^{-4} Ω·cm was obtained in a $(TiO_2)_x$ $(ZnO)_{100-x}$ film with x = 2 wt.%, this film also showed an excellent transmittance with an average of over 85.% in the visible range with a wide band gap, which were comparable to those of ITO. In addition, TZO films were found to be electrically and optically stable when they were exposed to a hydrogen plasma. On the other hand, TZO films with x = 2 wt.% were also deposited on the polyethylene naphthalate (PEN) substrates. It was found that the electrical resistivity of the films was greatly influenced by the applied RF-power and the vaporizations of moisture and organic solvents the diffused from the substrates in the sputtering process. If a proper buffer layer is coated on the PEN to suppress the diffusion of vapors from the substrate, a TZO film with an improved quality might be obtained, The TZO film on deposited on PEN is also found to be electrically stable against the bending stress as compared with that of ITO film. We, therefore, suggest that TZO films are sufficiently transparent and have a high enough conductivity and a high stability when exposed to the hydrogen plasma so that they can be applied to TCO films for displays and thin-film solar cells.

Funding

This work was supported by research grants from the Catholic University of Daegu in 2013.

References

[1] Minami, T., Kakumu T., & Takata, S. J. (1996). *Vac. Sci. Technol. A*, *14*, 1704.
[2] Hiramatsu, H., Seo, W. S., & Koumoto, K. (1998). *Chem. Mater.*, *10*, 3033.
[3] Yan, Y., Pennycook, S. J., Dai, J., Chang, R. P. H., Wang, A., & Marks, T. J. (1998). *Appl. Phys. Lett.*, *73*, 2585.
[4] Minami, T. J. (1999). *Vac. Sci. Technol. A*, *17*, 1765.
[5] Minami, T., Miyata, T., & Yamamoto, T. J. (1999). *Vac. Sci. Technol. A*, *17*, 1822.
[6] Chopra, K. L., Major, S., & Pandya, D. K. (1983). *Thin Solid Films*, *102*, 1.
[7] Takata, S., Minami, T., & Nanto, H. (1986). *Thin Solid Films*, *135*, 183.
[8] Minami, T., Takata, S., Kakumu, T., & Sonohara, H. (1995). *Thin Solid Films*, *270*, 22.
[9] Minami, T., Sonohara, H., Kakumu, T., & Takata, S. (1995). *Jpn. J. Appl. Phys.*, *34*, L971.
[10] Park, S. H., Kim, H. M., Rhee, B. R., & Gho, E. Y. (2001). *Jpn. J. Appl. Phys.*, *40*, 1429.

[11] Manifacier, J. C., Gasiot, J., & Fillard, J. P. J. (1976). *Phys. E*, *9*, 1002.
[12] Hsiung, J. E. J. (1990). *Electron. Mater.*, *25*, 1806.
[13] Tao, G. (1994). *Sol. Energy Mater. Sol. Cell.*, *34*, 359.
[14] Kaijou, A., Ohyama, M., Shibata, M., & Inoue, K. (1999). *United States Patent*, Patent No. 5, *972*, 527.
[15] Huh, K.S., Hong, H.J., Lee, E.W., Park, S.Y., Jeon, C. W., & Lee, S.H. (2010). *Mol. Cryst. Liq. Cryst.*, Vol. *532*, 65.
[16] Chopra, K. L., & Pandya, D. K. (1983). *Thin Solid Films*, *102*, 1.
[17] Jung, Y.S., Choi, H.W., Kim, K.H., & Bare, C.W. (2012). *Mol. Cryst. Liq. Cryst.*, Vol. *566*, 80.
[18] Pei, Z. L., Sun, C., Tan, M. H., Xiao, J. Q., Huang, R. F., & Wen, L. S. J. (2001). *Appl. Phys.*, *907*, 3432.
[19] Furuta, M., Hiramatsu, T., Matsuda, T., Furuta, H., & Hirao, T. (2007). *Jpn. J. Appl. Phys.*, *46*, 4038.
[20] Tabuchi, K., Wenas, W. W., Yamada, A., & Kakahashi, K. (1993). *Jpn. J. Appl. Phys.*, *132*, 3764.
[21] An, I., Lu, Y., Wronski, C. R., & Collins, R. W. (1994). *Appl. Phys. Lett.*, *64*, 3317.
[22] Lamp, U., & Muller, J. (1989). *Sens. Actuators*, *18*, 269.
[23] Horsthuis, W. H. G. (1989). *Thin Solid Films*, *147*, 185.
[24] Honda, S., Jimoto, A. T., Watamori, M., & Oura, K. (1995). *J. Vac. Sci. Technol.*, *133*, 1100.
[25] Hamberg, I., & Granqvist, C. G. J. (1986). *Appl. Phys.*, *60*, R123.
[26] Cminami, L., Nanto, H., & Takada, S. (1984). *Jpn. J. Appl. Phys.*, *23*, 1280.
[27] Park, J.-M., Hong, J.-S., Kim, J.-J., Park, S.-H., Kim, H.-M., & Ahn, J.-S. J. (2006). *Korean Phys. Soc.*, *48*, 1530.
[28] Park, J. M., Kim, J. J., Kim, H. M., Kim, J. H., Ryu, S. W., Park S. H., & Ahn, J. S. J. (2006). *Korean Phys. Soc.*, *48*, 1624.